allowing the energy to be determined by the quantum numbers of the field alone.

The authors' satisfaction with the scheme has been increased by the accident that it was first developed using an older compilation[10] with fewer particles. When applied to the newer list, it proved capable of classifying nearly all the particles by filling gaps in the older sequences.

Lack of a method to predict any properties of the particles other than the masses sometimes leaves the assignment in doubt. In such cases particles are assigned to more than one sequence.

[10] A. H. Rosenfeld, A. Barbaro-Galtieri, W. H. Barkas, P. L. Bastien, J. Kirz, and M. Roos, Rev. Mod. Phys. 37, 633 (1965).

PHYSICAL REVIEW VOLUME 163, NUMBER 5 25 NOVEMBER 1967

# Radiative Decays of $K^*$ Mesons*

MICHAEL SAPIR AND PAUL SINGER
*Department of Physics, Technion, Israel Institute of Technology, Haifa, Israel*
(Received 17 July 1967)

A general analysis of the first-order radiative decays of $K^*$ mesons, namely, $K^*\to K\gamma$, $K^*\to K\pi\gamma$, and $K^*\to K\pi\pi\gamma$, is presented. The main emphasis is on the decay processes $K^{*+}\to K^+\pi^0\gamma$, $K^{*+}\to K^0\pi^+\gamma$, $K^{*0}\to K^+\pi^-\gamma$, and $K^{*0}\to K^0\pi^0\gamma$, which reveal the electromagnetic structure of $K^*$ mesons. These decays can proceed through inner bremsstrahlung as well as direct emission, and they turn out to be the principal $K^*$ radiative processes. The inner-bremsstrahlung contribution results in a decay probability of approximately 1% of the strong decay for $\gamma$ rays with energies exceeding 10 MeV. The variation of the probability with the value of the $K^*$ magnetic moment is calculated. The direct decays are shown to be generally several orders of magnitude weaker. The decay $K^{*0}\to K^0\pi^0\gamma$ is the only channel in which the two mechanisms are comparable.

## 1. INTRODUCTION

THE $K^*$ charged and neutral vector mesons (mass $=892.4\pm0.8$ MeV/$c^2$) have been observed so far since their discovery in 1961,[1] only through their main decay mode, caused by strong interactions, into a kaon and a pion. Radiative decays of $K^*$ caused by the electromagnetic interactions are also expected to occur at a measurable, though obviously less frequent rate. Recent experiments[2] have already been dealing with fairly large samples of $K^*$ mesons, of the order of 5000 events, thus making it feasible to explore rare decay modes. Moreover, direct detection of radiative decay modes of vector mesons has also been attempted. For instance, the search[3] for the $\rho\to\pi\gamma$ decay has yielded an upper limit of 0.6 MeV for the partial width of this decay mode.

In this article we present a theoretical treatment of the first-order (in the fine structure constant $\alpha=1/137$) radiative decays of the $K^*$ charged and neutral mesons. The possible decays in this class are: (a) $K^*\to K\gamma$; (b) $K^*\to K\pi\gamma$; (c) $K^*\to K\pi\pi\gamma$.

In general, a radiative decay of particle $A$, namely $A\to\sum_i B_i+\gamma$, where $B_i$ are massive particles, can be caused by any or both of the following mechanisms: "internal bremsstrahlung" and "direct emission." In the first case, the emission of the photon is due to one of the incoming or outgoing particles participating in the strongly allowed process $A\to\sum_i B_i$, while the "direct" decay reflects the internal structure of the interactions of the decaying particle. The decay $K^*\to K\gamma$ is a "direct" decay, while $K^*\to K\pi\gamma$ and $K^*\to K\pi\pi\gamma$ can occur through both mechanisms.

Only a short discussion will be devoted to the decays $K^*\to K\gamma$ and $K^*\to K\pi\pi\gamma$. The first one has been treated theoretically also by previous authors, and the second one is expected to be very rare. We shall concentrate mainly on a detailed analysis of the decays $K^*\to K\pi\gamma$.

From our calculations it turns out that these latter decays are expected to be at least as frequent as, and for some channels even more frequent than, the $K^*\to K\gamma$ radiative decays. Their detailed study will help one to learn about the electromagnetic interactions of the $K^*$ vector mesons, as well as to check the validity of the higher symmetries prevailing in particle interactions. The latter point will, however, reveal itself sometimes only in a model-dependent way. One of the features we have investigated and which deserves special mention is the possibility of learning about the magnetic moments of charged and neutral $K^*$ mesons from the radiative decays $K^*\to K\pi\gamma$. As the measurement of this fundamental property by other methods

* Based in part on a thesis by Michael Sapir submitted to the Senate of the Technion, Israel Institute of Technology, in partial fulfillment of the requirements for the degree of Master of Science.

[1] M. Alston, L. W. Alvarez, P. Eberhard, M. L. Good, W. Graziano, H. K. Ticho, and S. M. Wojcicki, Phys. Rev. Letters 6, 300 (1961).

[2] J. H. Friedman and R. R. Ross, Phys. Rev. Letters 16, 485 (1966).

[3] G. Fidecaro, M. Fidecaro, J. A. Poirier, and P. Schiavon, Phys. Letters 23, 163 (1966).

seems to be very difficult, the results we obtain in this connection are of particular significance. The interest in the magnetic moments of $K^*$'s is also stimulated by the fact that by symmetry considerations their magnitudes are related to those of other vector mesons, as well as to the strength of the magnetic dipole transition "vector meson $\to$ pseudoscalar meson$+\gamma$." At least one of the latter category, the $\omega\to\pi\gamma$ partial decay width, is known experimentally.

## 2. THE DECAY MODES $K^*\to K\gamma$ AND $K^*\to K\pi\pi\gamma$

The $K^*\to K\gamma$ decay is a magnetic dipole transition, and it can be related to other similar decays of vector mesons by symmetry assumptions. The simplest form of the effective Lagrangian for this $V\to P+\gamma$ process is

$$\mathfrak{L}_{VP\gamma}=(f_{VP\gamma}/m)\epsilon^{\alpha\beta\gamma\delta}\partial_\alpha V_\beta{}^\dagger\partial_\gamma A_\delta P+\text{H.c.}, \qquad (1)$$

where $V$, $A$, $P$ stand for the vector, electromagnetic, and pseudoscalar fields, and $f_{VP\gamma}$ is a dimensionless coupling constant. By assuming for this Lagrangian $SU(3)$ symmetry plus singlet-octet mixing in the nonet picture,[4] the following relations[5] are obtained for the transition amplitudes: $(\varphi|\pi\gamma)=0$;

$$\begin{aligned}(\omega|\pi\gamma)=3(\rho|\pi\gamma)=3\sqrt{3}(\omega|\eta\gamma)&=\sqrt{3}(\rho|\eta\gamma)\\ =(3\sqrt{3}/2\sqrt{2})(\varphi|\eta\gamma)&=3(K^{*+}|K^+\gamma)\\ &=(-\tfrac{3}{2})(K^{*0}|K^0\gamma). \qquad (2)\end{aligned}$$

The same relations can be derived by assuming the $SU(6)$ symmetry scheme.[6]

The decay width for $K^*\to K\gamma$ obtained from (1) is

$$\Gamma_{K^*}(K\gamma)=\frac{f_{K^*K\gamma}{}^2}{4\pi}\frac{(m_{K^*}{}^2-m_K{}^2)^3}{24m^2m_{K^*}{}^3}. \qquad (3)$$

The $\gamma$-ray energy in this decay is 306 MeV. By using the measured value $\Gamma_\omega(\pi\gamma)=1.2$ MeV,[7] one obtains $(f_{\omega\pi\gamma}{}^2/4\pi)=0.17\alpha$ if $m$ is taken to be equal to the pion mass. Keeping the same $m$ for all the transitions involved, the relations (2) apply accordingly to the $f_{VP\gamma}$'s and then

$$f_{K^{*+}K^+\gamma}{}^2/4\pi=0.019\alpha,\quad f_{K^{*0}K^0\gamma}{}^2/4\pi=0.076\alpha. \qquad (4)$$

Using these values and the masses given in Ref. 7 (we take $m_{K^{*0}}=m_{K^{*+}}=892.4$ MeV$/c^2$), one obtains

$$\Gamma_{K^{*+}}(K^+\gamma)=75.3\text{ keV},\quad \Gamma_{K^{*0}}(K^0\gamma)=294\text{ keV}. \qquad (5)$$

Compared to the main decay mode, $\Gamma_{K^*}(K\pi)=49.8$ MeV, one has

$$\begin{aligned}\frac{\Gamma_{K^{*+}}(K^+\gamma)}{\Gamma_{K^{*+}}(K^+\pi^0+K^0\pi^+)}&=0.15\%,\\ \frac{\Gamma_{K^{*0}}(K^0\gamma)}{\Gamma_{K^{*0}}(K^0\pi^0+K^+\pi^-)}&=0.59\%.\end{aligned} \qquad (6)$$

The figures given previously in the literature[8] are one order of magnitude lower. This was probably due to the inadvertent use of a formula like (3) with $m=m_K$, after fixing $f_{\omega\pi\gamma}$ from an expression with $m=m_\pi$. As the relations (2) stand for the amplitudes, they connect the ratios $f_{VP\gamma}/m$. One could try indeed to take into account breaking of the symmetries assumed in (2), and in this case one might assume different values of $m$, with the $f$'s related by (2). Experimental deviations from (6) could decide whether this is necessary, and whether this is the right way of treating symmetry breaking. In any case, as the physical masses are used in our calculations, the phase-space aspect of symmetry breaking is already taken into account. A quark-model calculation of these decays by Rubinstein, Scheck, and Socolow[9] gives a ratio $r=\Gamma_{K^{*0}}(K^0\gamma)/\Gamma_{K^{*+}}(K^+\gamma)$ of the order of 2, instead of our result of approximately 4. Hence, its measurement could indeed prove an interesting test for the two approaches. The absolute values obtained in Ref. 9 for these partial widths are of the same order of magnitude as ours.

The decay $K^*\to K\pi\pi\gamma$ could occur either as "direct" emission or as an "inner bremsstrahlung" accompanying the strong $K^*\to K\pi\pi$ decay. This latter decay has been estimated by several authors[8,10,11] to have a partial decay width $\Gamma_{K^*}(K\pi\pi)\simeq 5$–$10$ keV. The "inner-bremsstrahlung" part is expected to be less than 1% of the decay it accompanies, while the "direct decays" are usually even less frequent. Hence, one can safely estimate

$$\Gamma_{K^*}(K\pi\pi\gamma)/\Gamma_{K^*}(K\pi)<10^{-4}\%, \qquad (7)$$

and we shall henceforth not embark on a detailed discussion of this very rare decay mode.

## 3. CONTRIBUTIONS TO THE DECAY AMPLITUDES FOR $K^*\to K\gamma\pi$

In dealing with the radiative decays $K^*\to K\pi\gamma$, one has to consider the following four possibilities:

$$K^{*0}\to K^++\pi^-+\gamma, \qquad (8a)$$

$$K^{*0}\to K^0+\pi^0+\gamma, \qquad (8b)$$

$$K^{*+}\to K^++\pi^0+\gamma, \qquad (8c)$$

$$K^{*+}\to K^0+\pi^++\gamma. \qquad (8d)$$

[4] S. Okubo, Phys. Letters **5**, 165 (1963).
[5] This kind of relations, assuming $SU(3)$ only, were first considered by N. Cabibbo and R. Gatto [Nuovo Cimento **21**, 872 (1961)].
[6] L. D. Soloviev, Phys. Letters **16**, 345 (1965).
[7] A. H. Rosenfeld, A. Barbaro-Galtieri, W. J. Podolsky, L. R. Price, P. Soding, C. G. Wohl, M. Roos, and W. J. Willis, Rev. Mod. Phys. **39**, 1 (1967).
[8] J. Yellin, Phys. Rev. **147**, 1080 (1966).
[9] H. R. Rubinstein, F. Scheck, and R. H. Socolow, Phys. Rev. **154**, 1608 (1967).
[10] M. Sweig, Phys. Rev. **131**, 860 (1963).
[11] D. Griffiths and D. Welling, Phys. Rev. Letters **14**, 874 (1965).

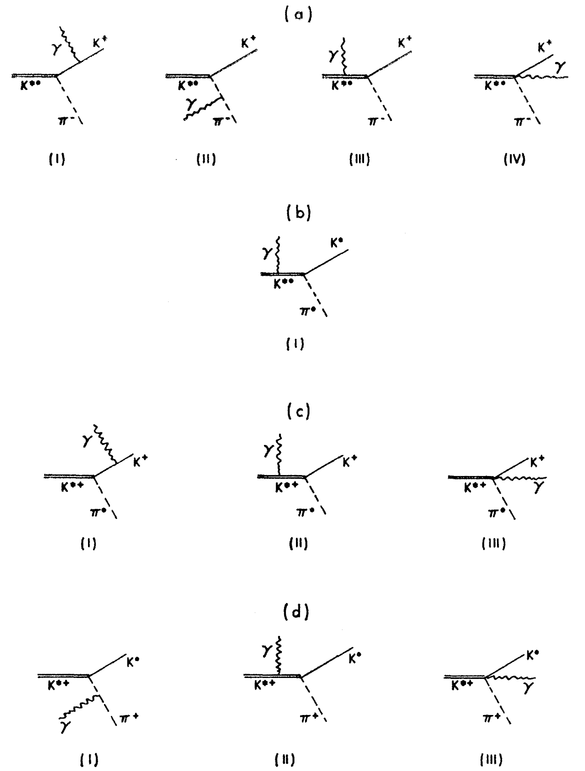

FIG. 1. Feynman diagrams representing the inner-bremsstrahlung contribution to the $K^* \to K\pi\gamma$ amplitudes: (a) $K^{*0} \to K^+\pi^-\gamma$; (b) $K^{*0} \to K^0\pi^0\gamma$; (c) $K^{*+} \to K^+\pi^0\gamma$; (d) $K^{*+} \to K^0\pi^+\gamma$.

For each of these four processes there is an "inner-bremsstrahlung" part, with the $\gamma$ ray emitted by the incoming $K^*$ or the outgoing kaon and pion from the strong process $K^* \to K+\pi$. This part of the amplitude can be calculated essentially in a manner, independent of any particular model, by using the rules of quantum electrodynamics. In addition, there will be a "direct" emission, which can be estimated by assuming a specific model. In this chapter we describe our approach to calculating the $K^* \to K\pi\gamma$ amplitude, using both mechanisms, and we start with the inner-bremsstrahlung part.

The Feynman diagrams illustrating the inner bremsstrahlung amplitudes are given in Fig. 1 for the four processes (8a)–(8d). The Hamiltonian of the $K^*K\pi$ strong interaction is

$$H_{\text{int}}^{K^*K\pi} = (\tfrac{1}{2}\sqrt{2}) f_{K^*K\pi}[K^\dagger \tau_i K_\mu{}^* \partial_\mu \pi_i - (\partial_\mu K^\dagger)\tau_i K_\mu{}^* \pi_i] + \text{H.c.}, \quad (9)$$

where the fields are denoted with the appropriate particle nomenclature. $K$ and $K_\mu{}^*$ are spinors in isotopic-spin space and $\tau_K$ are the isotopic-spin matrices. Greek letters (running from 0 to 3) are used for Lorentz indices and Latin letters (running from 1 to 3) for isotopic-spin indices.

The combination with the plus sign of the two terms appearing in (9) is eliminated by the requirement for the vector field to obey $\partial_\mu K_\mu{}^* = 0$. We take $f_{K^*K\pi}$ to be constant, and no form-factor dependence is allowed for the particles being off their mass shell in the processes of Fig. 1. This point will be taken up again in the last chapter.

The interaction Hamiltonian with the electromagnetic field of the charged pseudoscalar and vector particles involved is built to obey the principle of minimal electromagnetic inteaction.[12] To first order in $e$ it has the form

$$\begin{aligned} H_{\text{int}}{}^{\text{e.m.}} = {} & ieA_\mu[(\partial_\mu \pi^\dagger)\pi - \pi^\dagger(\partial_\mu \pi)] \\ & + ieA_\mu[(\partial_\mu K^\dagger)K - K^\dagger(\partial_\mu K)] \\ & + ieA_\mu[K_\nu{}^{*\dagger}(\partial_\mu K_\nu{}^* - \partial_\nu K_\mu{}^*) \\ & - K_\nu{}^*(\partial_\mu K_\nu{}^{*\dagger} - \partial_\nu K_\mu{}^{*\dagger})] + ie\chi F_{\mu\nu} K_\mu{}^{*\dagger} K_\nu{}^*, \quad (10) \end{aligned}$$

where $F_{\mu\nu} = \partial_\mu A_\nu - \partial_\nu A_\mu$ and $\chi$ is the "anomalous" magnetic moment of the $K^*$ charged meson. The total magnetic moment of the spin-one $K^*$ meson is given by

$$\mu = \frac{e\hbar(1+\chi)}{2m_{K^*}c}. \quad (11)$$

$\chi$ and $e$ are the two independent parameters characterizing the electromagnetic interaction of a vector meson in the minimal form. The quadrupole moment is completely determined by these two parameters. This holds, of course, only in the absence of strong interaction. The latter ones could give rise to form factors and also induce effective terms not of the minimal type. The most general expression for the interaction of a vector boson with a photon, assumed to be $C$, $P$, and $T$ invariant, contains indeed three terms.[13] The third term, not appearing in (10), has a higher power dependence on external momenta than the one exhibited by the terms in (10), and contributes to the static electric quadrupole moment. Throughout this work we have used the minimal expression given in (10), with no form factors to multiply the $e$ and $\chi$ parameters.

Among the neutral particles participating in reactions (8a)–(8d), only the $K^{*0}$ can have electromagnetic structure. Assuming that it possesses a magnetic moment $\mu_0 = e\hbar\chi_0/2m_{K^*}c$, the interaction Hamiltonian is given by

$$H'_{\text{int}}{}^{\text{e.m.}} = ie\chi_0 F_{\mu\nu} K_\mu{}^{*0} K_\nu{}^{*0}. \quad (12)$$

We now turn to describing the model we propose for calculating the direct contributions to the decays $K^* \to K\pi\gamma$. The basic approach is to take into account the contributions of the lowest mass states connected to the channel under treatment, in a dispersion-theoretic sense. In order to analyze our amplitude, let us consider the scattering process $K^* + \bar{K} \to \pi + \gamma$, which is the analytic continuation of the decay under study. The three channels connected by crossing symmetry

[12] See, e.g., T. D. Lee, Phys. Rev. 140, B967 (1965).
[13] V. Glaser and B. Jaksic, Nuovo Cimento 5, 1197 (1957).

are in our case

$$s\text{ channel: } K^*+\bar{K}\rightarrow\pi+\gamma\,, \tag{13a}$$

$$u\text{ channel: } K^*+\bar{\pi}\rightarrow K+\gamma\,, \tag{13b}$$

$$t\text{ channel: } K^*+\gamma\rightarrow K+\pi\,. \tag{13c}$$

The poles and continuum contributions to these processes are as follows.

(a) The $s$ channel: There is one pole at $s=m_\pi^2$ when the intermediate state is charged, and no pole otherwise. The continuum contribution starts at $s=4m_\pi^2$ with two-pion states. Angular-momentum conservation forbids $S$ waves, and we shall approximate the allowed $P$ waves by the $\rho$ meson. $D$-wave pions also imply $D$ wave for the $K^*\bar{K}$ state, and this would require very high $s$, in order to contribute significantly. As we assume that high-energy contributions can be omitted, we neglect contributions from two-pion states with the angular momentum equal and higher than 2. The next contribution in this channel, from three-pions, starts at $9m_\pi^2$. This will be included by considering the $\omega$ and $\varphi$ mesons. Cuts arising from states higher than three-pions are disregarded for the $s$ channel.

(b) The $u$ channel: There is again one pole, now at $u=m_K^2$ when the intermediate state is charged, and no pole otherwise. The continuum starts at $u=(m_K+m_\pi)^2$ with $K\pi$ states. Again we take only $P$ waves into consideration ($S$ waves being forbidden), and these will be approximated by the $K^*$ meson. The higher three-particle states, starting at $(m_K+2m_\pi)^2$, are neglected.

(c) The $t$ channel: There is no pole in this channel, and the continuum starts with $K\pi$ states. We approximate this again by using a $K^*$, while higher states are consistently neglected.

The $\pi$ and $K$ poles arising in the $s$ and $u$ channel, as well as the quasipole in the $t$ channel represented by $K^*$, are exactly the contributions to the decays arising as inner bremsstrahlung, which are depicted in Fig. 1. The rest of the contributions, arising from the various lowest multiparticle states and representing the direct part, are all replaceable in our case by vector mesons. This simplifies our calculations considerably, and also allows us to use symmetry considerations to relate the various amplitudes. It turns out that we can in fact express our direct decays in terms of two coupling constants only ($f_{VVP}$ and $f_{VP\gamma}$), which are related to measured quantities by symmetry relations. The Feynman diagrams illustrating the "direct" contributions to the decay amplitudes, are given in Fig. 2.

To summarize, by analyzing in a Mandelstam-like approach the analytic structure of the amplitude for $K^*\rightarrow K\pi\gamma$ continued to the appropriate scattering process, we have exposed the relevant singularities.

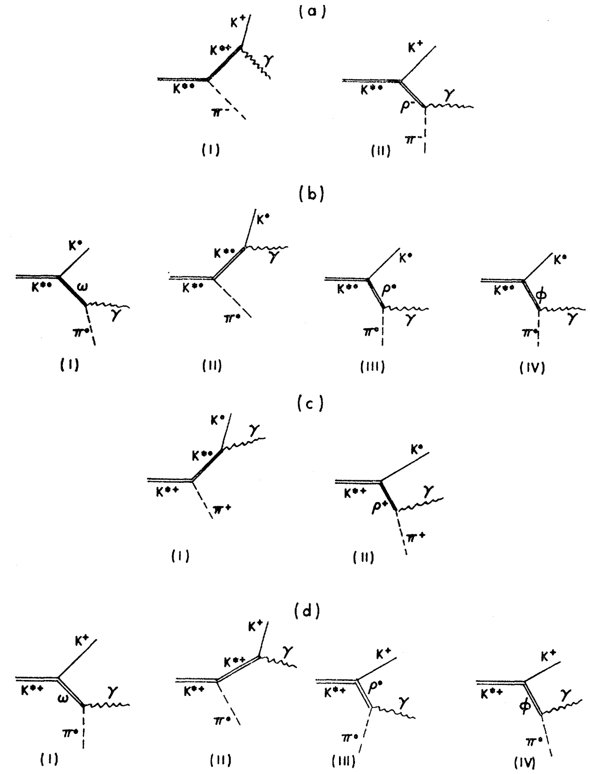

FIG. 2. Feynman diagrams representing the direct contribution to the $K^*\rightarrow K\pi\gamma$ amplitudes: (a) $K^{*0}\rightarrow K^+\pi^-\gamma$; (b) $K^{*0}\rightarrow K^0\pi^0\gamma$; (c) $K^{*+}\rightarrow K^0\pi^+\gamma$; (d) $K^{*+}\rightarrow K^+\pi^0\gamma$.

The pole terms are related to the inner-bremsstrahlung part, while the continuum cuts relate to the direct part. Of the latter, we use only the lowest-mass contributions, which can be approximated in our case by vector mesons.

## 4. CALCULATIONS

When calculating the decay widths for the processes (8a)–(8d), we find that the inner-bremsstrahlung part gives the main contribution to all but the $K^{*0}\rightarrow K^0+\pi^0+\gamma$ decay. We have therefore chosen to calculate separately the contribution to the rate arising from the inner bremsstrahlung and direct terms, i.e., we have neglected the interference term. Another reason for this procedure is the fact that the direct-part calculation is obviously model-dependent. Hence, one would like to have the two contributions separately for a first comparison with experiment. When enough experimental information is assembled, the further refinement of the calculations to include the interference term might be desirable. In the following, we shall denote by $M(\Gamma)$ and $M'(\Gamma')$ the invariant amplitudes (partial decay rates) for the inner bremsstrahlung and direct part, respectively.

The inner-bremsstrahlung amplitudes for the processes (8a)–(8d), depicted in Fig. 1(a)–(d), are

$$M_1 = e f_{K^*K\pi}\bigg\{ \epsilon^{(K^*)}\cdot(p_K-p_\pi)\bigg[\frac{p_\pi\cdot\epsilon^{(\gamma)}}{p_\pi\cdot k}-\frac{p_K\cdot\epsilon^{(\gamma)}}{p_K\cdot k}\bigg] - \epsilon^{(K^*)}\cdot k\bigg[\frac{p_\pi\cdot\epsilon^{(\gamma)}}{p_\pi\cdot k}+\frac{p_K\cdot\epsilon^{(\gamma)}}{p_K\cdot k}\bigg]+\frac{\Delta\chi_0}{2p\cdot k} \times[\epsilon^{(K^*)}\cdot k\epsilon^{(\gamma)}\cdot p-\epsilon^{(K^*)}\cdot\epsilon^{(\gamma)}p\cdot k] +2\epsilon^{(K^*)}\cdot\epsilon^{(\gamma)}+\frac{\chi_0}{2p\cdot k}[(p_K-p_\pi)\cdot k\epsilon^{(K^*)}\cdot\epsilon^{(\gamma)} -(p_K-p_\pi)\cdot\epsilon^{(\gamma)}k\cdot\epsilon^{(K^*)}]\bigg\}, \quad (14a)$$

$$M_2=\frac{e f_{K^*K\pi}\chi_0}{2\sqrt{2}p\cdot k}\{(p_K-p_\pi)\cdot k\epsilon^{(K^*)}\cdot\epsilon^{(\gamma)} -(p_K-p_\pi)\cdot\epsilon^{(\gamma)}k\cdot\epsilon^{(K^*)}+\Delta[\epsilon^{(K^*)}\cdot k\epsilon^{(\gamma)}\cdot p -\epsilon^{(K^*)}\cdot\epsilon^{(\gamma)}p\cdot k]\}, \quad (14b)$$

$$M_3=\frac{e f_{K^*K\pi}}{\sqrt{2}}\bigg\{-\epsilon^{(K^*)}\cdot(p_K-p_\pi+k)\frac{p_K\cdot\epsilon^{(\gamma)}}{p_K\cdot k} +\frac{p\cdot\epsilon^{(\gamma)}}{2p\cdot k}[2\epsilon^{(K^*)}\cdot(p_K-p_\pi)+\Delta(1-\chi)\epsilon^{(K^*)}\cdot k] -\frac{\epsilon^{(K^*)}\cdot\epsilon^{(\gamma)}}{2p\cdot k}[p\cdot(p_K-p_\pi+\Delta k) +\chi k\cdot(p_K-p_\pi-\Delta p)]+\epsilon^{(K^*)}\cdot\epsilon^{(\gamma)}\bigg(1+\frac{\Delta m_{K^*}^2}{2p\cdot k}\bigg) +\frac{1+\chi}{2p\cdot k}\epsilon^{(K^*)}\cdot k\epsilon^{(\gamma)}\cdot(p_K-p_\pi)\bigg\}. \quad (14c)$$

$$M_4=\sqrt{2}M_3 \quad (\text{with interchanging } p_K\rightleftarrows p_\pi;\, m_K\rightleftarrows m_\pi), \quad (14d)$$

with

$$\Delta\equiv(m_K^2-m_\pi^2)/m_{K^*}^2.$$

$p$, $k$ are the four-momenta of the $K^*$ meson and of the photon, respectively. It should be clarified here, that what we call the inner-bremsstrahlung part includes also a contribution which in some sense is of "direct" nature. We refer by this to the Feynman diagrams given in Fig. 1 under (a IV), (c III), (d III). Without these terms, the radiative amplitudes for the respective processes (a), (c), and (d) are not gauge invariant. These terms, which supplement the amplitude to a gauge-invariant expression, are obtained by replacing $p^{(+)}\rightarrow p^{(+)}-e\epsilon^{(\gamma)}$ and $p^{(-)}\rightarrow p^{(-)}+e\epsilon^{(\gamma)}$ in the expression of the strong vertex, and amount, therefore, to direct emission from the vertex, as it is indeed depicted in Fig. 1. The mere existence of this type of term is due to the momentum dependence of the strong vertex [Eq. (9)]. The diagrams which we classify under direct amplitudes (like those in Fig. 2) are *not related* by gauge invariance to the inner-bremsstrahlung terms like the terms we have just discussed. The truly direct terms are gauge-invariant taken alone, and they arise because of the additional inner structure of the vertices. The diagrams we include under this category given in Fig. 2 are an example of this type, and from the discussion of the analytic structure of the radiative amplitude we believe they are also the most significant ones.

In order to calculate the diagrams of Fig. 2 we use for the electromagnetic vertex the expression given in (1), while for the strong vertex we use

$$\mathcal{L}_{VVP}=\frac{f_{VVP}}{m}\epsilon^{\mu\nu\sigma\tau}\,\mathrm{Tr}(P\partial_\mu V_\nu\partial_\sigma V_\tau). \quad (15)$$

Here $V$ and $P$ stand for the vector nonet and the pseudoscalar octet, respectively, and the trace summation refers to the $SU(3)$ structure. Then the form of the invariant amplitude in the rest system of the decaying $K^*$ is

$$M'=\frac{f_{VP\gamma}f_{VVP}m_{K^*}}{(2m_{K^*}E^{(1)}-t^2)m^2}\epsilon_\mu{}^{(K^*)}\epsilon_\delta{}^{(\gamma)}k_\gamma p_\tau{}^{(1)}(p-p^{(1)})_\alpha \times\epsilon^{0\mu\tau\nu}\epsilon^{\alpha\gamma\delta\nu}, \quad (16)$$

where

$$t^2=m_{K^*}{}^2-m_V{}^2+m_{P^{(1)}}{}^2. \quad (17)$$

Here $E^{(1)}$, $p^{(1)}$, $m_{P^{(1)}}$ denote the energy, four-momentum, and mass of the pseudoscalar meson emitted at the strong vertex, and $m_V$ is the mass of the intermediate vector meson.

The inner-bremsstrahlung $\gamma$ spectrum is infrared divergent, while the direct spectrum goes to zero when the photon energy vanishes. Hence, we shall conveniently express the partial width for a certain $K^*\rightarrow K+\pi+\gamma$ inner-bremsstrahlung decay, as the relative probability for emitting a photon with energy greater than $k$, compared to the partial decay width of the appropriate strong channel

$$R_k(K^*\rightarrow K\pi\gamma)=\frac{\Gamma_{K^*}(K\pi\gamma)}{\Gamma_{K^*}(K\pi)}. \quad (18)$$

In Table I we give $R_k$ for the four processes (8a)–(8d). We have varied $\chi$ and $\chi_0$ between $-3$ and 3. For $K^{*0}\rightarrow K^0\pi^0\gamma$, the rate for $\chi_0\neq 1$ is obtainable from the values given in Table I by multiplying by $\chi_0^2$. The $\gamma$ spectrum for this decay is not infrared divergent as in the other three processes, as the only contribution arises from the possible magnetic moment of $K^{*0}$.

The formulas leading to Table I were checked against the appropriate expressions of Singer[14] and Iwao[15] for the decay $\rho\rightarrow\pi\pi\gamma$ by taking $m_{K^*}\rightarrow m_\rho$, $m_K\rightarrow m_\pi$ and were found to agree.

[14] P. Singer, Phys. Rev. **130**, 2441 (1963); **161**, 1694 (1967).
[15] S. Iwao, Nuovo Cimento **30**, 656 (1963).

TABLE I. The relative probabilities $R_k=\Gamma_{K^*}(K\pi\gamma)/\Gamma_{K^*}(K\pi)$, for the various decay channels, for emitting an inner-bremsstrahlung photon with energy greater than $k$.

| Mode | $\chi\chi_0$ \ $k$ (MeV) | 10 | 30 | 50 | 80 | 100 | 125 | 160 | 175 | 200 |
|---|---|---|---|---|---|---|---|---|---|---|
| $K^{*0}\rightarrow K^++\pi^-+\gamma$ | $-3$ | $10.5\times10^{-3}$ | 5.51 | 3.50 | 1.91 | 1.29 | 0.76 | 0.29 | 0.18 | 0.048 |
| | $-2$ | $10.5\times10^{-3}$ | 5.52 | 3.51 | 1.93 | 1.32 | 0.78 | 0.31 | 0.19 | 0.054 |
| | $-1$ | $10.5\times10^{-3}$ | 5.56 | 3.54 | 1.97 | 1.35 | 0.81 | 0.32 | 0.21 | 0.061 |
| | 0 | $10.6\times10^{-3}$ | 5.60 | 3.59 | 2.01 | 1.39 | 0.85 | 0.35 | 0.23 | 0.068 |
| | 1 | $10.6\times10^{-3}$ | 5.66 | 3.65 | 2.06 | 1.44 | 0.89 | 0.37 | 0.25 | 0.074 |
| | 2 | $10.7\times10^{-3}$ | 5.73 | 3.72 | 2.13 | 1.50 | 0.94 | 0.39 | 0.27 | 0.085 |
| | 3 | $10.8\times10^{-3}$ | 5.82 | 3.80 | 2.20 | 1.56 | 1.00 | 0.42 | 0.30 | 0.094 |
| $K^{*0}\rightarrow K^0+\pi^0+\gamma$ | 1 | $7.57\times10^{-6}$ | 7.22 | 6.61 | 5.33 | 4.38 | 3.17 | 1.61 | 1.18 | 0.33 |
| $K^{*+}\rightarrow K^++\pi^0+\gamma$ | $-3$ | $10.5\times10^{-4}$ | 6.01 | 4.18 | 2.70 | 2.05 | 1.43 | 0.81 | 0.53 | 0.19 |
| | $-2$ | $9.98\times10^{-4}$ | 5.48 | 3.69 | 2.27 | 1.69 | 1.15 | 0.64 | 0.40 | 0.14 |
| | $-1$ | $9.59\times10^{-4}$ | 5.10 | 3.33 | 1.96 | 1.41 | 0.92 | 0.50 | 0.30 | 0.10 |
| | 0 | $9.36\times10^{-4}$ | 4.87 | 3.11 | 1.76 | 1.22 | 0.77 | 0.40 | 0.22 | 0.072 |
| | 1 | $9.27\times10^{-4}$ | 4.79 | 3.02 | 1.67 | 1.13 | 0.68 | 0.33 | 0.17 | 0.048 |
| | 2 | $9.35\times10^{-4}$ | 4.86 | 3.07 | 1.68 | 1.13 | 0.66 | 0.30 | 0.14 | 0.033 |
| | 3 | $9.59\times10^{-4}$ | 5.08 | 3.26 | 1.82 | 1.22 | 0.70 | 0.30 | 0.13 | 0.025 |
| $K^{*+}\rightarrow K^0+\pi^++\gamma$ | $-3$ | $5.93\times10^{-3}$ | 3.07 | 1.92 | 1.04 | 0.67 | 0.35 | 0.14 | 0.09 | 0.017 |
| | $-2$ | $5.93\times10^{-3}$ | 3.07 | 1.92 | 1.05 | 0.68 | 0.37 | 0.15 | 0.10 | 0.020 |
| | $-1$ | $5.94\times10^{-3}$ | 3.09 | 1.94 | 1.06 | 0.70 | 0.38 | 0.16 | 0.11 | 0.024 |
| | 0 | $5.98\times10^{-3}$ | 3.12 | 1.97 | 1.09 | 0.73 | 0.41 | 0.18 | 0.12 | 0.028 |
| | 1 | $6.02\times10^{-3}$ | 3.16 | 2.01 | 1.13 | 0.76 | 0.43 | 0.20 | 0.13 | 0.033 |
| | 2 | $6.07\times10^{-3}$ | 3.22 | 2.06 | 1.18 | 0.81 | 0.44 | 0.22 | 0.15 | 0.038 |
| | 3 | $6.14\times10^{-3}$ | 3.29 | 2.13 | 1.24 | 0.86 | 0.49 | 0.25 | 0.17 | 0.044 |

The "direct" part of the decays was calculated by using the diagrams of Fig. 2 with the amplitudes having the form given in Eq. (16). The electromagnetic vertices $VP\gamma$ are related to each other as given in Eq. (2) and their absolute value gauged from the $\omega\rightarrow\pi\gamma$ decay as explained in Sec. 2.

The various $f_{VVP}$ couplings are related through the assumptions of $SU(3)$ invariance plus the nonet picture for vector mesons, and Eq. (15) implies the following relations:

$$\begin{aligned}f_{VVP}&=f_{K^{*+}K^{*0}\pi^+}=f_{K^{*+}\rho^+K^0}=\sqrt{2}f_{K^{*+}\omega K^+}\\&=\sqrt{2}f_{K^{*+}K^{*+}\pi^0}=\sqrt{2}f_{K^{*+}\rho^0K^+}=f_{K^{*+}\varphi K^+}\\&=f_{K^{*0}K^{*+}\pi^-}=f_{K^{*0}\rho^-K^+}=\sqrt{2}f_{K^{*0}\omega K^0}\\&=-\sqrt{2}f_{K^{*0}K^{*0}\pi^0}=f_{K^{*0}\varphi K^0}=-\sqrt{2}f_{K^{*0}\rho^0K^0}\\&=\tfrac{1}{2}\sqrt{2}f_{\omega\rho\pi}.\end{aligned}\tag{19}$$

The $f_{\omega\rho\pi}$ coupling is obtained, assuming the $\omega\rightarrow3\pi$ decay proceeds[16] through the $\omega\rightarrow\rho\pi\rightarrow3\pi$ sequence. Taking the mass constant appearing in (15) to be $m=m_\pi$, one has

$$f_{\omega\rho\pi}^2/4\pi=0.68.\tag{20}$$

It could well be that the $\omega\rightarrow3\pi$ decay proceeds only partially through the Gell-Mann–Sharp–Wagner mechanism,[16] the rest being due to a direct four-meson ($\omega3\pi$) vertex.[11] In this case, the value given in (20) should be lowered by a factor of approximately 2, decreasing even more the expected contributions of direct decays.

The numerical values we obtain for the various partial decay widths for "direct" decays are as follows:

$$\Gamma'(K^{*0}\rightarrow K^+\pi^-\gamma)/\Gamma(K^{*0}\rightarrow K^+\pi^-)=1.42\times10^{-6},\tag{21a}$$

$$\Gamma'(K^{*0}\rightarrow K^0\pi^0\gamma)/\Gamma(K^{*0}\rightarrow K^0\pi^0)=6.00\times10^{-6},\tag{21b}$$

$$\Gamma'(K^{*+}\rightarrow K^0\pi^+\gamma)/\Gamma(K^{*+}\rightarrow K^0\pi^+)=7.12\times10^{-6},\tag{21c}$$

$$\Gamma'(K^{*+}\rightarrow K^+\pi^0\gamma)/\Gamma(K^{*+}\rightarrow K^+\pi^0)=3.12\times10^{-6}.\tag{21d}$$

To obtain these numerical values for the decays summarized in Fig. 2, we used for $f_{VP\gamma}$ and $f_{VVP}$ the numerical values implied in Eqs. (2), (4), (19), and (20).

## 5. DISCUSSION AND CONCLUSIONS

Our calculations show that the $K\pi\gamma$ decay mode of $K^*$ is its most frequent radiative decay process. The calculated occurrence turns out to be as high as 1% of the strong decay for photon energies larger than 10 MeV. This figure refers to processes (8a), (8c), and (8d). On the other hand, the two-body process $K^*\rightarrow K\gamma$ which is favored by phase space, is expected to be less frequent than the three-body decay $K^*\rightarrow K\pi\gamma$ by a factor varying between 2 to 10 [see (Eq. 6)] for the various channels considered. This strength of the $K^*\rightarrow K\pi\gamma$ channel is due to the inner-bremsstrahlung mechanism, which strongly favors the low-energy photon emission. The direct-part contribution to $K^*\rightarrow K\pi\gamma$ is small [see Eq. (21)], amounting only to 0.01% of the inner-bremsstrahlung part for $K^{*0}\rightarrow K^+\pi^-\gamma$ (with $k>10$ MeV). For charged $K^*$ decays, although the figure climbs to approximately 0.1%, it is still insignificant.

The exception to the above summary is the $K^{*0}\rightarrow K^0\pi^0\gamma$ decay. In this case, the inner-bremsstrahlung

[16] M. Gell-Mann, D. Sharp, and W. G. Wagner, Phys. Rev. Letters 8, 261 (1962).

part is due only to the possible existence of a $K^{*0}$ magnetic moment, and if it has a value of the order of one Bohr magneton, a rate of the order of $10^{-5}$ to the main decay is expected. The direct decay is then of comparable magnitude [Eq. (21b)].

It should be remarked that similar results have been obtained previously for $\rho \to \pi\pi\gamma$ decay,[14] where the inner-bremsstrahlung part is also some 1% of the $\rho \to 2\pi$ decay, although in that case the direct contribution was found to be somewhat more significant.[17]

Relations among the various $V \to P+P'+\gamma$ amplitudes have been previously obtained by Tanaka[18] in the framework of $SU(6)$ symmetry. The relations obtained in Ref. 18 are for the direct amplitudes, although this is not explicitly stated throughout the paper. These relations are different from those we obtained by using our model, which is $SU(3)$-symmetric with breaking due to $\omega$-$\varphi$ mixing in the nonet picture. For instance, Tanaka obtains

$$\langle K^{*0} | \pi^- K^+ \gamma \rangle = \langle K^{*+} | \pi^+ K^0 \gamma \rangle = 0$$

and

$$\langle K^{*+} | K^+ \pi^0 \gamma \rangle = \langle K^{*0} | K^0 \pi^0 \gamma \rangle .$$

It can be easily checked that these relations are not consistent with our model by inspecting Fig. 2 and Eqs. (2) and (19). Hence, a measurement of the direct part might distinguish between our model and the exact $SU(6)$ predictions. Unfortunately, as the direct part is expected to be very minute, such a test seems to be quite remote from the experimental point of view.

Proceeding to details of our calculations, the differences between the values obtained for the different processes (8a), (8c), and (8d) and given in Table I can be easily understood. The strength of the inner-bremsstrahlung radiation is inversely proportional to the mass-squared of the radiating charged particle. Hence, the process $K^{*0} \to K^+ + \pi^- + \gamma$ is the strongest one, while $K^{*+} \to K^0 + \pi^+ + \gamma$ is already weaker as $K^0$ is not radiating. The $K^{*+} \to K^+ + \pi^0 + \gamma$ is the weaker of the three, namely by one order of magnitude compared to $K^{*+} \to K^0 + \pi^+ + \gamma$. This is indeed the ratio of the squared masses of the pion and kaon. The radiation coming from $K^{*+}$ is again appropriately weaker, so as not to seriously affect these rough considerations.

The $\gamma$-ray spectrum is essentially given in Table I, and for illustration we plot it in Fig. 3 for the $K^{*0} \to K^+\pi^-\gamma$ process (the inner-bremsstrahlung part). There is obviously a large preponderance of low-energy photons. On the other side, the direct-emission photon spectrum vanishes for $k \to 0$, and it has large probability for high-energy photons. The direct spectrum for the same

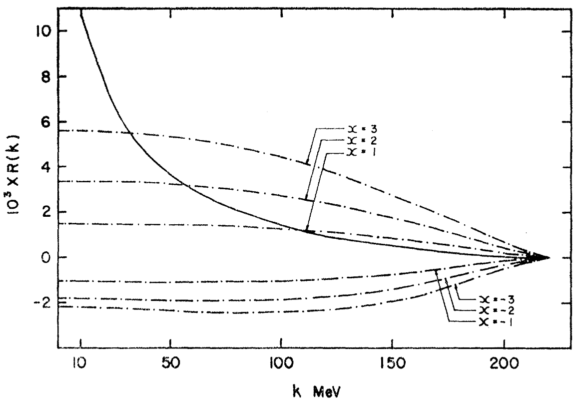


FIG. 3. The relative probability $R_k = [\Gamma_{K^{*0}}(K^+\pi^-\gamma)/\Gamma_{K^{*0}}(K^+\pi^-)]$ for emission of an inner-bremsstrahlung photon with energy exceeding $k$ MeV. The continuous line is for $\chi=0$; the broken lines represent the additional contribution to $R_k$ for various values of $\chi$, magnified by a factor of 25. The magnetic moment is $\mu = e\hbar(1+\chi)/2m_{K^*}c$.

$K^{*0} \to K^+\pi^-\gamma$ process is given in Fig. 4, and it rises to a maximum at $k_0 = 197$ MeV, very close to its upper end ($k_{\max} = 221$ MeV). As the probability for the direct part is very small (at least with our model), one would expect the experimental findings to follow the spectrum of Fig. 3, with possible distortions due to direct emission occurring only for high-energy ($k > 150$ MeV) photons.

In calculating the Feynman diagrams of Fig. 1, we assumed no form-factor dependence. One should have taken into account that the strong matrix element entering the diagrams is not to be taken with all the particles on the mass shell. What permits us to neglect this correction is the low-energy theorem for radiative decay amplitudes.[19] If we write for the inner-bremsstrahlung spectrum the form

$$F(k) = A/k + B + Ck + \cdots , \qquad (22)$$

it can be easily shown, following Chew, that $A$ and $B$ are determined by the amplitude for the strong process $K^* \to K\pi$. As the overwhelming part of the contribution comes from these terms, we are entitled to the procedure we followed. This, of course, does not hold for the direct part, where possible off-mass-shell effects for the vertices involved might cause deviations from the values given in (21). However, this can happen in any case because of symmetry breaking of relations (2) and (19).

An additional factor which could affect the spectra and was neglected here entirely is the $K$-$\pi$ rescattering effects.

Let us now turn to a discussion of the magnetic moments of $K^*$, whose possible measurement via radiative processes was one of the stimuli for the present work.

$SU(3)$ symmetry predicts equal magnetic moments for the charged $\rho$ and $K^*$ mesons, i.e., $\mu_{K^{*+}} = \mu_{\rho^+}$ and

[17] In Ref. 14 the direct part to $\rho^{+,0} \to \pi\pi\gamma$ was calculated for several values of the $\omega\rho\pi$ coupling constant, as the experimental width of $\omega$ was still unknown at that time. The presently measured value is very close to the figure used in the second row of Table II of Ref. 14 [i.e., $\Gamma_\omega(3\pi) = 11$ MeV].

[18] K. Tanaka, Phys. Rev. **142**, 1087 (1966).

[19] H. Chew, Phys. Rev. **123**, 377 (1961).

zero magnetic moment for the $K^{*0}$ meson,[20] i.e., $\chi_0=0$. By assuming a specific model, namely the vector-meson dominance of the vector-meson electromagnetic vertex, Flamm obtains $\chi_{K^{*+}}=\chi_{\rho^+}=1$, i.e., a magnetic moment of two magnetons, and $\chi_0$ still zero, although $K^{*0}$ develops electromagnetic structure.

Soloviev[6] has discussed the magnetic moment of vector mesons within the $SU(6)$ symmetry scheme and derived relations between the magnetic moments and the transition amplitudes $V\rightarrow P+\gamma$, as the 9 vector mesons and 8 pseudoscalar mesons belong now to the same 35-dimensional multiplet. He obtains

$$\mu(K^{*+})=\mu(\rho^+)=(\omega|\pi\gamma), \tag{23}$$

which supplements Eq. (2). By using the known experimental value of $(\omega|\pi\gamma)$, Eq. (23) predicts for $\mu(K^*)$ a value of 2.5–3 magnetons.

Some predictions about the $\mu(K^{*0})$ have been obtained by considering the medium-strong interaction breaking the $SU(3)$ and $SU(6)$ symmetry. Babaev *et al.*[21] obtain several relations, when various assumptions are made about the symmetry-breaking terms. One of their relations reads for instance

$$\mu(K^{*0})=\tfrac{1}{2}[\mu(\rho^+)-\mu(K^{*+})]. \tag{24}$$

Because of expected symmetry breaking, this could indeed be as high as 0.2–0.5 magneton. One might remark in this connection that Dalitz and Sutherland[22] have shown that the $M1$ photoexcitation amplitude $p\rightarrow N^{*+}$ does definitely deviate from the $SU(6)$ predicted value.

We have therefore performed our calculations with

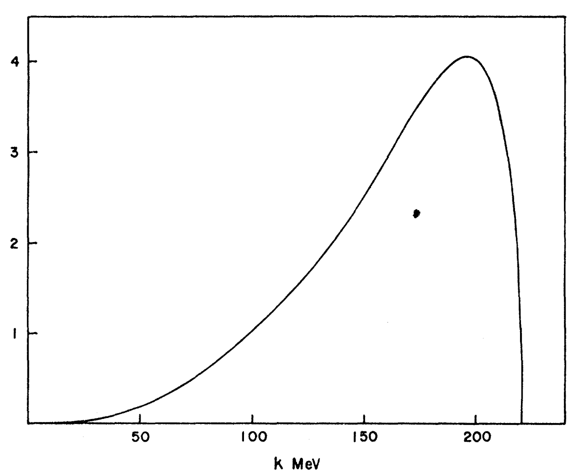


FIG. 4. The energy spectrum of a direct photon in the decay $K^{*0}\rightarrow K^++\pi^-+\gamma$.

[20] D. Flamm, Nuovo Cimento **38**, 291 (1965).
[21] Z. R. Babaev, V. S. Zamiralov, and L. D. Soloviev, Zh. Eksperim. i Teor. Fiz., Pis'ma v Redaktsiyu **2**, 314 (1965) [English transl.: Soviet Phys.—JETP Letters **2**, 199 (1965).
[22] R. H. Dalitz and D. G. Sutherland, Phys. Rev. **146**, 1180 (1966).

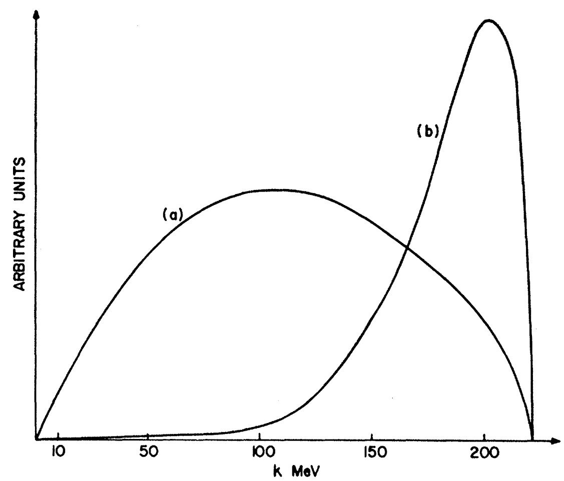


FIG. 5. The photon energy spectra from the decay $K^{*0}\rightarrow K^0\pi^0\gamma$: (a) due to $K^{*0}$ magnetic moment; (b) due to direct emission. The ratio of the integrated spectra is normalized to the values given in Eqs. (25) and (21b).

$\chi$ and $\chi_0$ as parameters which were changed between $-3$ and 3. The effect of $\chi$ varies from channel to channel. For $K^{*0}\rightarrow K^++\pi^-+\gamma$ a change of one magneton induces a change in the decay width ranging from 1% for $R(k>30$ MeV) to 10% for $R(k>175$ MeV). For $K^{*+}\rightarrow K^0+\pi^++\gamma$ the changes are slightly larger, while for $K^{*+}\rightarrow K^++\pi^0+\gamma$ they reach 3% for $R(k>30$ MeV) to 20% for $R(k>175$ MeV). The trouble is that the high-energy part of the $\gamma$ spectrum, which is sensitive to the value of the magnetic moment, is also the region where the small amount of direct amplitude concentrates its contribution. The detailed numerical results are summarized in Table I.

Of particular interest is the decay $K^{*0}\rightarrow K^0+\pi^0+\gamma$. In this case, for $\chi_0=1$, we obtain

$$\Gamma_{K^{*0}}(K^0\pi^0\gamma)/\Gamma_{K^{*0}}(K^0\pi^0)=7.8\times10^{-6}, \tag{25}$$

while for $\chi_0=3$ one has $6.5\times10^{-5}$ for the above ratio. Here the direct decay was found [Eq. (21b)] to contribute $\Gamma_{K^{*0}}'(K^0\pi^0\gamma)/\Gamma_{K^{*0}}(K^0\pi^0)=6\times10^{-6}$. Therefore, a measurement of this mode would be very fruitful. In Fig. 5 we present the $\gamma$-ray spectra for the two mechanisms (again, no estimate of the interference has been made).

In conclusion, one should realize that only extensive measurements of the $K^*\rightarrow K\pi\gamma$ mode could bring the desired information on the $K^*$ magnetic moments. The alternative suggestion of Berman and Drell[23] for getting this information, namely the forward photoproduction of vector mesons via vector-meson exchange, is also a very difficult experimental task. It seems therefore that painstaking experiments of both radiative decay and photoproduction kind will be needed in order to reveal the electromagnetic structure of vector mesons.

[23] S. M. Berman and S. D. Drell, Phys. Rev. **133**, B791 (1964); S. M. Berman and U. Maor, Nuovo Cimento **36**, 483 (1965).